CORA Cork Open Research Archive
Cartlann Taighde Oscailte Chorcaí

Title	Dual wavelengths inverse spatially offset Raman spectroscopy for bone characterization
Authors	Ma, Hui;Gautam, Rekha;Konugolu Venkata Sekar, Sanathana;O'Flynn, Carrie;Henn, Patrick;Andersson-Engels, Stefan
Publication date	2023-03-06
Original Citation	Ma, H., Gautam, R., Konugolu Venkata Sekar, S., O'Flynn, C., Henn, P. and Andersson-Engels, S. (2023) 'Dual wavelengths inverse spatially offset Raman spectroscopy for bone characterization', Proceedings of SPIE, 12368, Advanced Biomedical and Clinical Diagnostic and Surgical Guidance Systems XXI, 123680A (4pp). doi: 10.1117/12.2650089
Type of publication	Conference item
Link to publisher's version	10.1117/12.2650089
Rights	© 2023, Society of Photo-Optical Instrumentation Engineers (SPIE). One print or electronic copy may be made for personal use only. Systematic reproduction and distribution, duplication of any material in this paper for a fee or for commercial purposes, or modification of the content of the paper are prohibited.
Download date	2026-11-04 17:10:12
Item downloaded from	https://hdl.handle.net/10468/14422

UCC
University College Cork, Ireland
Coláiste na hOllscoile Corcaigh

PROCEEDINGS OF SPIE

SPIEDigitalLibrary.org/conference-proceedings-of-spie

Dual wavelengths inverse spatially offset Raman spectroscopy for bone characterization

Hui Ma, Rekha Gautam, Sanathana Konugolu Venkata Sekar, Carrie O'Flynn, Patrick Henn, et al.

Hui Ma, Rekha Gautam, Sanathana Konugolu Venkata Sekar, Carrie O'Flynn, Patrick Henn, Stefan Andersson-Engels, "Dual wavelengths inverse spatially offset Raman spectroscopy for bone characterization," Proc. SPIE 12368, Advanced Biomedical and Clinical Diagnostic and Surgical Guidance Systems XXI, 123680A (6 March 2023); doi: 10.1117/12.2650089

SPIE.

Event: SPIE BiOS, 2023, San Francisco, California, United States

Downloaded From: https://www.spiedigitallibrary.org/conference-proceedings-of-spie on 01 May 2023 Terms of Use: https://www.spiedigitallibrary.org/terms-of-use

Dual wavelengths inverse Spatially Offset Raman Spectroscopy for bone characterization

Hui Ma*[a,b], Sanathana Konugolu Venkata Sekar[a], Pranav Lanka[a], Carrie O'Flynn[c], Patrick Henn[c], Stefan Andersson-Engels[a,b], Rekha Gautam[a]
[a]Tyndall National Institute, Lee Maltings Complex, Dyke Parade, T12R5CP, Cork, Ireland;
[b]Department of Physics, University College Cork, College Road, Cork, T12 K8AF, Ireland;
[c]ASSERT Centre, University College Cork, College Road, Cork, T12 K8AF, Ireland

ABSTRACT

Osteoporosis is a disease that weakens bones increasing the possibility of bone fracture. The gold standard to diagnose osteoporosis is measuring bone mineral density (BMD). Since BMD only partly determines the strength of the bone, more information on chemical composition and microstructure is needed. Here, we implemented a novel dual-wavelength inverse Spatially Offset Raman Spectroscopy (SORS) to characterize tissue chemical composition covering both the fingerprint and high-wavenumber regions. This system provides a greater probing depth keeping the spectrometer setting constant. The results from hydroxyapatite (HA) and water phantom demonstrate the potential of the Raman system to assess bone mineral and matrix quality *in-vivo*.

Keywords: Osteoporosis, Raman, SORS, BMD, Hydration

1. INTRODUCTION

Osteoporosis is a disease that weakens bones, making them fragile and brittle, and increases the possibility of bone fracture. In 27 European Union countries plus Switzerland and the UK, 25.5 million women and 6.5 million men were estimated to be influenced by osteoporosis in 2019. There are 4.3 million osteoporosis-related fragility fractures every year which leads to an economic burden of €56 billion[1]. Thus, early diagnosis of osteoporosis is crucial for guiding appropriate and timely intervention. Osteoporosis is diagnosed when the bone mineral density (BMD) is 2.5 SDs (Standard deviations) or more below the average value of young healthy women[2]. The clinical reference standard to measure BMD is dual-energy X-ray absorptiometry (DXA). However, BMD values partly determines the strength of the bone[3]. The information on organic matrix and microstructure is missing. That explains the low accuracy in fracture risk prediction under some circumstances, like the measurements on early postmenopausal women and type 2 diabetes patients[4, 5]. The optical method is an emerging option to provide a low cost and minimally invasive non-ionizing radiation-based diagnosis method for osteoporosis.

Raman spectroscopy has been considered a real-time non-destructive optical method for characterising molecular information and chemical composition of materials including biological tissue. Compared to the conventional Raman spectroscopy, spatially offset Raman spectroscopy (SORS) can probe deep inside the turbid material due to the source detector separation[6]. In this study, SORS signals were acquired using a simple solution of changing the source detector distance by tuning the position of an axicon[7]. This approach also helped in reducing the photon density on the tissue allowing the use of optimum power to obtain better signal-to-noise ratio[8]. For comprehensive bone characterisation, mineral and matrix information were obtained from the fingerprint region (200-1800cm^{-1}), and hydration information can be acquired from the high wavenumber region (2700-4000cm^{-1}) using a dual wavelength light source. The dual-wavelength approach allows measuring fingerprint and high wavenumber regions without the use of any movable part keeping the setting of the spectrometer constant[9]. This dual-wavelength inverse SORS configuration proves the potential of Raman spectroscopy to characterise the bone mineral and matrix quality and hydration *in vivo*.

Advanced Biomedical and Clinical Diagnostic and Surgical Guidance Systems XXI,
edited by Caroline Boudoux, James W. Tunnell, Proc. of SPIE Vol. 12368,
123680A · © 2023 SPIE · 1605-7422 · doi: 10.1117/12.2650089

Downloaded From: https://www.spiedigitallibrary.org/conference-proceedings-of-spie on 01 May 2023
Terms of Use: https://www.spiedigitallibrary.org/terms-of-use

2. METHOD AND MATERIAL

2.1 Sample preparation

Gelatine phantoms were prepared by dissolving 10%, 20%, and 30% gelatine powder in deionized water. These phantoms contained 90%, 80%, and 70% of water. For hydroxyapatite (HA) phantoms, 5% and 8% of HA together with 10% gelatine was dissolved in deionized water. For both hydration phantoms and HA phantoms, intralipid and India ink were added as scattering and absorption materials. Overlying tissue mimicking phantoms were made from agarose, TiO_2, and melanin. The reduced scattering and absorption coefficients (μ_s' and μ_a) of tissue mimicking phantoms were optimized to 10 cm^{-1} and 0.1cm^{-1} respectively at 830nm using a time resolved diffused optical system.

2.2 Experimental setup

Figure 1(a) illustrates the dual wavelength inverse SORS system. The dual wavelength laser source (Innovative Photonics Solutions, model # 0811A100-B Fat Boy) provides 730 nm and 830 nm laser excitations. The ring illumination was generated by an axicon, and the ring size could be adjusted by changing the position of the axicon. The back scattered light was collected from the centre of the ring and sent to the detector (Acton LS 785, Teledyne Princeton Instruments). Figure 1(b) shows the mapping fingerprint and high wavenumber regions on the detector corresponding to the excitation wavelength. The grating wavelength range was set at 857 – 1014 nm, which covered 382 – 2191 cm^{-1} for 830 nm excitation and 2034 – 3840 cm^{-1} for 730 nm excitation.

2.3 Data acquisition and processing

Different thickness of tissue mimicking phantom was overlaid on top of the HA and hydration phantoms and phosphate band (960 cm^{-1}) was used as guiding star to determine the penetration depth. The relation between the penetration depth and the ring size was characterised using 3 mm, 5 mm, and 7 mm radius ring sizes. The power density was set to 2.87 mW/mm^2 at 730 nm and 5.09 mW/mm^2 at 830 mm. The acquisition time was 30 s for 730 nm and 20 s for 830 nm. Fluorescence background in the spectra was removed using Asymmetric Least Squares method with lambda=4 and p=0.00005 and vector normalization was used in data processing[10].

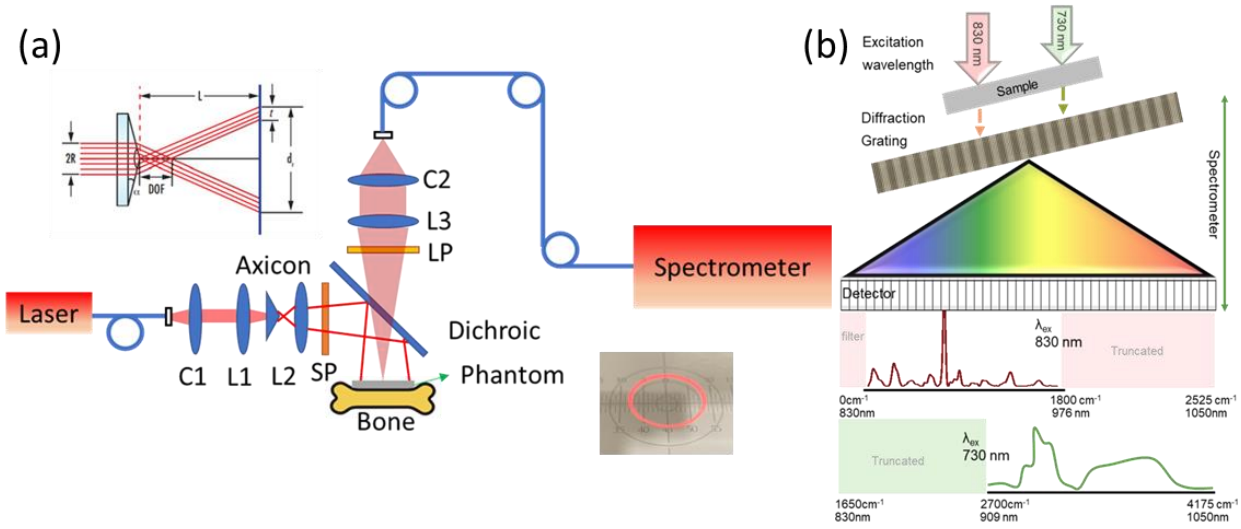


Figure 1. (a) Scheme of the Raman system. (C1, C2: collimators, L1, L2, L3: convex lenses, SP: short pass filter, LP: long pass filter. (b) Mapping fingerprint and high wavenumber regions on the detector corresponding to the excitation wavelength.

Downloaded From: https://www.spiedigitallibrary.org/conference-proceedings-of-spie on 01 May 2023
Terms of Use: https://www.spiedigitallibrary.org/terms-of-use

3. RESULT

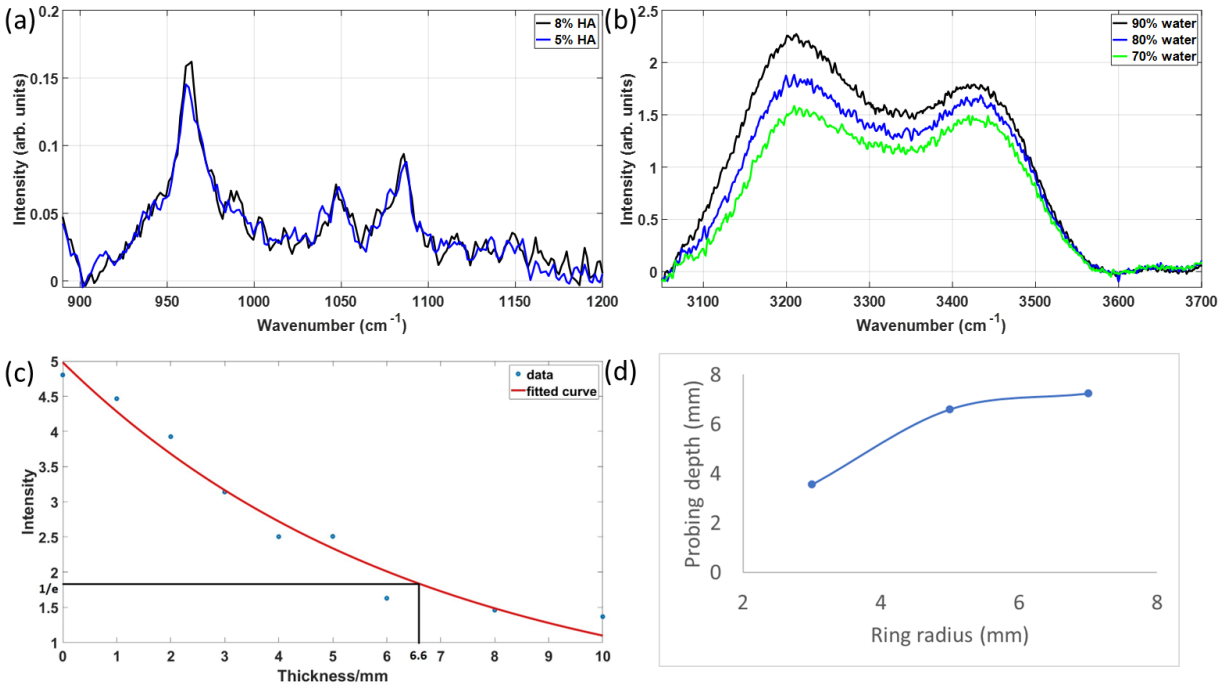


Figure 2. (a) Raman spectra of 8% and 5% HA phantoms under 5mm illumination ring radius and 5mm thick overlaid tissue mimicking phantom. (b) Raman spectra of 90%, 80%, and 70% water phantoms under 5 mm illumination radius. (c) The graph represents the decay in the signal intensity of phosphate peak (960 cm^{-1}) of 8% HA phantom with increase in thickness of the overlaid tissue mimicking phantoms acquired using 5 mm offset ring 8% HA phantom (d) The relation between the penetration depth and the radius for 8% HA phantom.

Figure 2. (a) shows that the illumination ring with 5 mm offset could differentiate the phosphate concentration of 5% and 8% HA when hidden underneath 5 mm tissue mimicking phantoms. Figure 2(b) illustrates that this system could also identify 10% difference in hydration. The penetration depth is calculated as the thickness of the overlaid tissue mimicking phantom when the intensity of the phosphate peak drops to 1/e of the HA phantom without overlaid phantom. Figure 2(c) shows that when the ring offset is 5 mm, the probing depth is 6.6 mm. From Figure 2(d) we can see the penetration depth increases when the illumination ring radius increases and then levels off. Since SNR drops as the radius increases, the 5 mm is considered as the optimum ring size. The depth sensitivity can further be improved by increasing the acquisition time.

4. DISCUSSION AND CONCLUSIONS

A system with 730 nm and 830 nm excitation wavelengths and an inverse SORS configuration using an axicon has been developed to cover fingerprint and high wavenumber regions of Raman spectra. The use of the inverse SORS configuration allows deeper probing than the conventional Raman spectroscopy. With 5 mm offset ring, we were able to measure signals as deep as 6.6mm and the attenuation is in line what would be expected for the light transport in tissue like phantom material. However, the depth of penetration levels off with further increase in offset due to loss in Raman signal strength (SNR). The addition of the high wavenumber region provides the quantitative information on hydration providing a comprehensive biochemical profile of bone mimicking phantoms . Further, the system was able to differentiate 3% change in HA and 10% change in hydration through tissue mimicking phantoms at a depth of 5 mm. This configuration is user-friendly and proves the potential of biomedical applications like bone characterisation.

Downloaded From: https://www.spiedigitallibrary.org/conference-proceedings-of-spie on 01 May 2023
Terms of Use: https://www.spiedigitallibrary.org/terms-of-use

REFERENCES

[1] Willers C, Norton N, Harvey NC, Jacobson T, Johansson H, Lorentzon M, et al. Osteoporosis in Europe: a compendium of country-specific reports. Archives of Osteoporosis. 2022;17(1):23.

[2] Kanis JA, Melton Iii LJ, Christiansen C, Johnston CC, Khaltaev N. The diagnosis of osteoporosis. Journal of Bone and Mineral Research. 1994;9(8):1137-41.

[3] Unal M, Creecy A, Nyman JS. The Role of Matrix Composition in the Mechanical Behavior of Bone. Current Osteoporosis Reports. 2018;16(3):205-15.

[4] Trémollieres FA, Pouillès JM, Drewniak N, Laparra J, Ribot CA, Dargent-Molina P. Fracture risk prediction using BMD and clinical risk factors in early postmenopausal women: sensitivity of the WHO FRAX tool. J Bone Miner Res. 2010;25(5):1002-9.

[5] Schwartz AV, Sellmeyer DE. Diabetes, fracture, and bone fragility. Current Osteoporosis Reports. 2007;5(3):105-11.

[6] Mosca S, Conti C, Stone N, Matousek P. Spatially offset Raman spectroscopy. Nature Reviews Methods Primers. 2021;1(1):21.

[7] Dépret Bt, Verkerk P, Hennequin D. Characterization and modelling of the hollow beam produced by a real conical lens. Optics communications. 2002;211(1-6):31-8.

[8] Matousek P. Inverse spatially offset Raman spectroscopy for deep noninvasive probing of turbid media. Applied spectroscopy. 2006;60(11):1341-7.

[9] Masson LE, O'Brien CM, Pence IJ, Herington JL, Reese J, Van Leeuwen TG, et al. Dual excitation wavelength system for combined fingerprint and high wavenumber Raman spectroscopy. Analyst. 2018;143(24):6049-60.

[10] Gautam R, Peoples D, Jansen K, O'Connor M, Thomas G, Vanga S, et al. Feature Selection and Rapid Characterization of Bloodstains on Different Substrates. Applied Spectroscopy. 2020;74(10):1238-51.

Downloaded From: https://www.spiedigitallibrary.org/conference-proceedings-of-spie on 01 May 2023
Terms of Use: https://www.spiedigitallibrary.org/terms-of-use